

A two-layer cellular automata model of carbon monoxide oxidation reaction*

Anastasia Kireeva

Abstract. A two-layer cellular automata (CA) model of carbon monoxide (CO) oxidation reaction on platinum is developed and investigated. The reaction in non-equilibrium conditions can be accompanied by various spatio-temporal patterns such as surface waves, spirals and turbulences. A two-layer CA is a parallel composition of the two CA – the main CA simulating the oxidation reaction and the second layer CA simulating a temperature spatiotemporal distribution on the catalyst surface. Using the second layer allows us to take into account changes of surface catalytic properties when temperature changes. In the process of the CA evolution, different spatial patterns on the catalyst surface with different temperature are obtained. Properties of patterns emerging for different temperature are revealed.

1. Introduction

The catalytic reaction of carbon monoxide (CO) oxidation on the platinum group metals is interesting both from practical and fundamental standpoints. In the catalytic reaction, different self-organization phenomena such as surface waves, spirals, rings and turbulence may appear. Moreover, the reaction dynamics depends on external factors: surface temperature, gas temperature and reagents partial pressure. Thus, the CO oxidation catalytic reaction is a complex nonlinear system. Studying such a system by differential equations is an extremely difficult task. A powerful method of complex nonlinear systems investigation is cellular automata simulation. A cellular automaton is a discrete model where space is represented by a finite set of cells, system dynamics is described by cells states evolution given by a transition rule. Cellular automata models of various physical, chemical, social phenomena are described and studied by many researchers [1–4] and others.

The CO oxidation reaction over platinum (Pt₁₀₀) surface is simulated by Monte Carlo method [5], which served as a basis for the CA model [6]. Such models use constant rates coefficients of reaction stages without allowance for the reaction dynamics with temperature changes.

A two-layer cellular automaton is used for simulating CO oxidation reaction allowing for surface temperature changes, which are simulated by the

*Supported by Russian Foundation for Basic Research under Grant 14-01-31425-mol-a (2014) and 12-03-00766-a, Siberian Branch of Russian Academy of Sciences, Interdisciplinary Project 47.

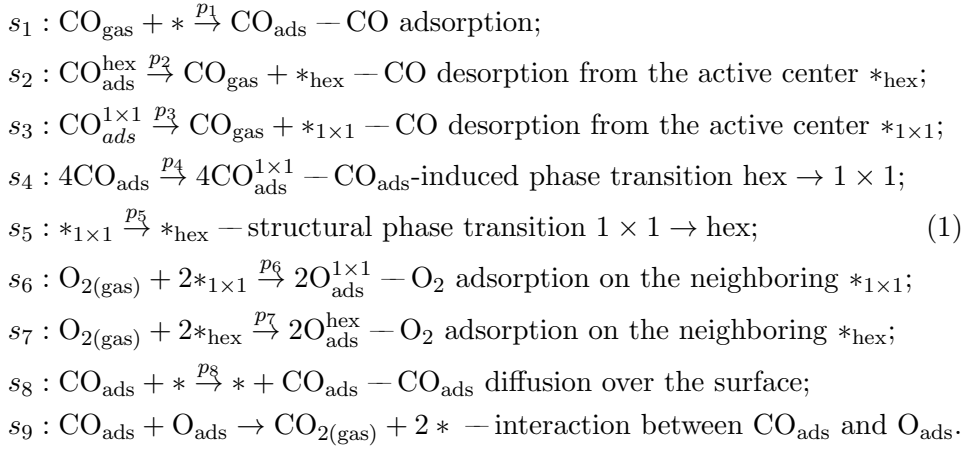
second layer. The first layer, i.e., the main CA simulates the reaction dynamics depending on surface temperature. Transition rules of the main CA depend on cells states of the second CA.

The aim of this research is developing the CO oxidation reaction over Pt catalyst CA-model allowing for surface temperature changes and studying the dynamics reaction for different temperature distributions.

In Section 1, the description of CO oxidation reaction mechanism and formulas for calculation of the rate coefficients depending on temperature are introduced. Section 2 describes a two-layer CA-model of the reaction — the main CA, the second layer CA and their transition rules. Results of CA simulation are presented in Section 3.

2. The mechanism of CO oxidation reaction over Pt₁₀₀

Experimental and theoretical studies show that in the course of the CO oxidation reaction, the Pt₁₀₀ surface being reconstructed from a cubic (1 × 1) to a hexagonal (hex) structure under the action of the adsorbed CO [7, 8]. In [5, 7], the following mechanism of the CO oxidation reaction over Pt₁₀₀ has been studied:



Here the symbols “*_{hex}”, “*_{1×1}” and “*” denote the vacant active center of the surface with hexagonal, cubic and an arbitrary structure (hex or 1 × 1), respectively. The symbols s_1 – s_9 denote elementary stages of the oxidation reaction.

According to the algorithm proposed in [5], the active centers of a catalyst surface are chosen at random, and one of the above-mentioned stages s_i is chosen with probability p_i calculated by the formula

$$p_i = \frac{k_i}{k}, \quad i = 1, \dots, 8, \quad k = \sum_{l=1}^8 k_l, \tag{2}$$

where k_i is a rate coefficient of the i th stage.

In [5], k_i , $i = 1, \dots, 7$, are constant values corresponding to the surface temperature $T = 480$ K, whereas in this paper, the rate coefficients depend on the surface temperature and are calculated by the Arrhenius equation

$$k_i = v_i \exp\left(-\frac{E_i}{RT}\right), \quad i = 2, 3, 4, 5, 8, \quad (3)$$

where v_i is a pre-exponential factor determined by the frequency of molecules collisions, E_i is the activation energy equal to the minimum energy required to start a chemical reaction, $R = 1.985875 \cdot 10^{-3}$ [kcal / (K · mol)] is the Universal gas constant and T is the absolute temperature on the Kelvin scale.

The values of v_i and E_i for the stages s_i , $i = 2, 3, 4, 5, 8$, of CO oxidation reaction specified in [9] are presented in the table:

	$i = 2$	$i = 3$	$i = 4$	$i = 5$	$i = 8$
v_i, s^{-1}	$4 \cdot 10^{13}$	$3 \cdot 10^{15}$	10^{15}	$5 \cdot 10^{11}$	$0.68 \text{ cm}^2/\text{s}$
$E_i, \text{kcal/mol}$	28.5	37.3	31.9	25	7

A pre-exponential factor of diffusion v_8 is specified in [9] as $0.68 \text{ cm}^2/\text{s}$. To compare v_8 with other pre-exponential factors, it should be evaluated in the s^{-1} units. In this paper, the pre-exponential factor of diffusion v_8 is taken about $6 \cdot 10^6 \text{ s}^{-1}$. The oscillations of reagents concentrations coinciding with [5] are obtained by computing experiments for this value of v_8 .

The rate coefficients k_1 , k_6 and $k_7 = k_6 \cdot 10^{-3}$ are determined by the partial pressure and do not depend on the surface temperature. The stage s_9 is realized immediately after CO and O adsorption or after diffusion if CO_{ads} and O_{ads} appear in the nearest neighbor.

3. The two-layer CA model of CO oxidation reaction over Pt

For simulating the CO oxidation reaction dynamics with the temperature influence, a two-layer CA is used. The two-layer CA is a parallel composition [10] of two cellular automata—the main CA (\aleph_{CO}) simulating the oxidation reaction and the CA of second layer (\aleph_T) simulating a temperature spatiotemporal distribution on the catalyst surface:

$$\aleph_S = \Upsilon(\aleph_{\text{CO}}, \aleph_T).$$

In the general case, a CA is defined by the four concepts [3, 10]: $\aleph = \langle A, X, \Theta, \mu \rangle$, where A is a cells *state alphabet*, X is the *set of names*, Θ is a *local operator*, μ is the operation mode. A *cell* is represented by a pair $(u, (i, j))$, where $u \in A$ is a cell state, $(i, j) \in X$ is a cell name. Alphabet A represents possible states of the investigated system. A set of names X

is a set of integer coordinates of cells in the discrete space corresponding to the system space. The local operator Θ defines the cells states updating rules according to the system behavior. The operation mode μ defines the order of the local operator Θ application to the cells $(i, j) \in X$. There are synchronous, asynchronous and block-synchronous operation modes. In the synchronous mode, a local operator is applied to all cells of a CA, all being updated simultaneously. The asynchronous mode of a CA prescribes the local operator to be applied to a randomly chosen cell, changing its state immediately. The block-synchronous mode is a transformation of the asynchronous one, which is used for achieving a high performance of the asynchronous CA parallel implementation.

3.1. The main CA simulating of the CO oxidation reaction over Pt is defined as follows:

$$\aleph_{\text{CO}} = \langle A_{\text{CO}}, X_{\text{CO}}, \Theta_{\text{CO}}, \alpha \rangle.$$

The state alphabet A_{CO} is chosen according to the reagents participating in reaction (1): $A = \{ *_{1 \times 1}, *_{\text{hex}}, \text{CO}_{\text{ads}}^{1 \times 1}, \text{CO}_{\text{ads}}^{\text{hex}}, \text{O}_{\text{ads}}^{1 \times 1}, \text{O}_{\text{ads}}^{\text{hex}} \}$, where $\text{CO}_{\text{ads}}^{1 \times 1}$ and $\text{CO}_{\text{ads}}^{\text{hex}}$ are carbon monoxide adsorbed on 1×1 and hex surfaces, $\text{O}_{\text{ads}}^{1 \times 1}$ and $\text{O}_{\text{ads}}^{\text{hex}}$ are oxygen adsorbed on 1×1 and hex surfaces, respectively.

The set of names $X_{\text{CO}} = \{(i, j) : i = 1, \dots, M_i, j = 1, \dots, M_j\}$ contains integer coordinates of cells in the discrete space corresponding to the catalyst surface. On X_{CO} , *naming functions* $\varphi(i, j) : X_{\text{CO}} \rightarrow X_{\text{CO}}$ are introduced. A naming function determines one of the neighbors for a cell with the name (i, j) . A set of naming functions determines an *underlying template* $T(i, j)$, defining the nearest neighbors of the cell (i, j) . In the CA model under investigation, the following templates are used (Figure 1):

$$T_k(i, j) = \{\varphi_0(i, j), \dots, \varphi_{k-1}(i, j)\}, \quad k = 1, 5, 9, 13, \quad (4)$$

where

$$\begin{aligned} T_{13}(i, j) = \{ & (i, j), (i, j - 1), (i + 1, j), (i, j + 1), (i - 1, j), \\ & (i - 1, j - 1), (i + 1, j - 1), (i + 1, j + 1), (i - 1, j + 1), \\ & (i, j - 2), (i + 2, j), (i, j + 2), (i - 2, j) \}. \end{aligned}$$

The local operator $\Theta_{\text{CO}}(i, j)$ defines the rules of cells states updating according to the stages of oxidation reaction (1), $\Theta_{\text{CO}}(i, j)$ is a system of substitutions θ_l , $l \in \{2, 3, 4, 5\}$, and their superpositions $\theta_{(l,9)} = \theta_9(\theta_l)$, $l \in \{1, 6, 7, 8\}$:

$$\Theta_{\text{CO}}(i, j) = \{\theta_{(1,9)}, \theta_2, \theta_3, \theta_4, \theta_5, \theta_{(6,9)}, \theta_{(7,9)}, \theta_{(8,9)}\}.$$

The application of $\Theta_{\text{CO}}(i, j)$ to the cell (i, j) consists in the choice of one of the substitutions either θ_l or $\theta_{(l,9)}$ with probability p_l (2) and calculation of the new states of cells in $T(i, j)$.

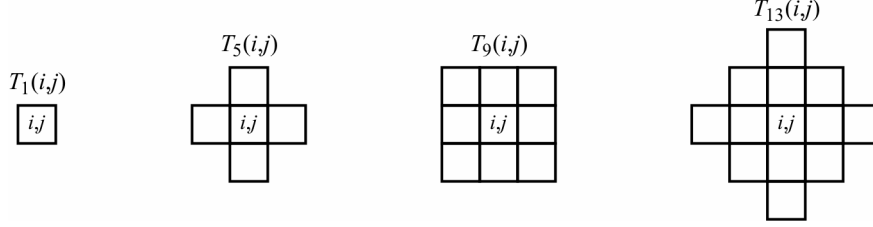


Figure 1. Underlying templates used in the CA-model of oxidation reaction

Each substitution $\theta_l \in \Theta_{\text{CO}}(i, j)$ corresponds to the elementary stage s_l . For example, oxygen adsorption is realized at the two neighboring active centers $*_{1 \times 1}$ as follows:

$$\theta_6(i, j) = \{(*_{1 \times 1}, (i, j))(*_{1 \times 1}, \varphi_k(i, j)) \xrightarrow{p_6} (O_{\text{ads}}^{1 \times 1}, (i, j))(O_{\text{ads}}^{1 \times 1}, \varphi_k(i, j))\},$$

$$k = 1, 2, 3, 4.$$

The interaction between CO_{ads} and O_{ads} is simulated by the substitution

$$\theta_9(i, j) = \{(\text{CO}_{\text{ads}}, (i, j))(O_{\text{ads}}, \varphi_k(i, j)) \rightarrow (*, (i, j))(*, \varphi_k(i, j))\},$$

$$k = 1, 2, 3, 4.$$

Here, the absence of the indices “ 1×1 ” and “hex” means that substitution is applied irrespective of the surface phase and does not change the surface structure.

For the application of $\theta_l \in \Theta_{\text{CO}}(i, j)$ the templates shown in Figure 1 are used. Particularly, substitutions θ_l , $l \in \{2, 3, 4, 5\}$, are applied to a single cell, hence the template $T_1(i, j)$ is used. The substitution θ_4 is applied to a block consisting of four neighboring cells. The block is chosen at random out of the template $T_9(i, j)$. For application of θ_l , $l \in \{6, 7, 8, 9\}$, two cells are required: (i, j) and one of its four neighbors $\varphi_k(i, j) \in T_5(i, j)$, $k = 1, 2, 3, 4$, is chosen with probability 0.25.

The application of $\theta_{(l,9)} = \theta_9(\theta_l)$, $l = 6, 7, 8$, is performed as follows. At first θ_l is applied to the cell (i, j) changing states of (i, j) and one of $\varphi_k(i, j) \in T_5(i, j)$, $k = 1, 2, 3, 4$. Immediately after the application of θ_l , θ_9 is applied to both (i, j) and $\varphi_k(i, j)$ cells using four neighbors of (i, j) and four neighbors of $\varphi_k(i, j)$. As a result, the application of $\theta_{(l,9)} = \theta_9(\theta_l)$, $l = 6, 7, 8$, requires to use the template $T_{13}(i, j)$:

$$T_{13}(i, j) = \bigcup_{k=1}^4 T_5(\varphi_k(i, j)).$$

The application of superposition $\theta_{(1,9)} = \theta_9(\theta_1)$ requires the template $T_5(i, j)$ since the substitution θ_1 changes the state of one cell, and then the

substitution θ_9 is applied to this cell, using one of four neighboring cells $\varphi_k(i, j) \in T_5(i, j)$, $k = 1, 2, 3, 4$.

The operation mode of \aleph_{CO} is asynchronous. The simulation process is divided into *iterations*. An iteration of \aleph_{CO} is $|X_{\text{CO}}| \cdot M_{\text{diff}}$ applications of the substitutions $\theta_l \in \Theta_{\text{CO}}(i, j)$ to randomly chosen cells $(i, j) \in X_{\text{CO}}$, M_{diff} being a parameter of CO diffusion intensity. The diffusion in the oxidation reaction occurs M_{diff} times more often than other chemical processes, therefore iteration of \aleph_{CO} is M_{diff} times increased. According to [5, 7], M_{diff} is selected in the range $50 \div 100$.

An iteration transfers the cellular array $\Omega(t)$ into $\Omega(t+1)$, where t is an iteration number. The sequence $\sum(\Omega) = \Omega(0), \dots, \Omega(t), \Omega(t+1), \dots, \Omega(t_{\text{fin}})$ is named *evolution*.

3.2. The CA simulating of the temperature spatiotemporal distribution on the catalyst surface is defined as follows:

$$\aleph_T = \langle A_T, X_T, \Theta_T, \alpha \rangle.$$

The state alphabet $A_T = \{u \in \mathbb{R}\}$ corresponds to values of the catalyst surface temperature. The set of names $X_T = \{(i, j) : i = 1, \dots, M_i, j = 1, \dots, M_j\}$ contains integer coordinates of cells in the discrete space corresponding to the catalyst surface. The underlying template of \aleph_T is $T_5(i, j)$ specified by (4).

The temperature spatiotemporal evolution on the catalyst surface is simulated by the multi-particle CA model for diffusion simulation [11], except for one feature. In \aleph_T , the cells states are real numbers as opposed to those in the multi-particle CA model, where cells states are integer numbers. The main idea of this CA model is as follows. A cell state is divided into two parts according to the value of γ : $u = (1 - \gamma)u + \gamma u$, where γ is a parameter determining the model diffusion rate, the neighboring cells exchanging values of their second parts.

The local operator Θ_T is determined on the basis of [11] as follows:

$$\begin{aligned} \Theta_T(i, j) &= \{(u, (i, j))(u_k, \varphi_k(i, j)) \rightarrow (u', (i, j))(u'_k, \varphi_k(i, j))\}, \\ k &= 1, 2, 3, 4, \quad u' = (1 - \gamma)u + \gamma u_k, \quad u'_k = (1 - \gamma)u_k + \gamma u. \end{aligned}$$

The operation mode of \aleph_T is asynchronous. An iteration of \aleph_T is $|X_T|$ applications of the local operator Θ_T to randomly chosen cells $(i, j) \in X_T$.

3.3. A parallel composition of \aleph_{CO} and \aleph_T . The dynamics of CO oxidation reaction depends on the catalyst surface temperature. In the course of the reaction a cooling down or heating of some parts of the surface proceeds. These temperature fluctuations cause a change in the reaction

properties of the catalyst. Hence, an inhomogeneous distribution of temperature over the catalyst surface produces different reaction rates for different parts of the surface. A two-layer CA enables one to simulate the reaction dynamics under such inhomogeneous changes in the catalyst properties.

As mentioned above, the two-layer CA \aleph_S is a parallel composition of the main CA \aleph_{CO} and CA of the second layer \aleph_T : \aleph_{CO} represents coverage of the surface by reagents and \aleph_T represents a temperature distribution over the catalyst surface. The parallel composition is defined in [10]. Between the names sets of \aleph_{CO} and \aleph_T there exists a one-to-one correspondence: $X_{CO} = \gamma(X_T)$. The cells states of \aleph_{CO} depend on the cells states of \aleph_T in the following way. The probability of $\theta_l \in \Theta_{CO}(i, j)$, $l = 1, \dots, 8$, application to the cell $(i, j) \in X_{CO}$ is a function of state of the second layer cell $(i, j) \in X_T$.

Thus, the simulation algorithm is as follows. The cell $(i, j) \in X_{CO}$ is randomly selected. For this, the cell corresponding to that of the second layer $(i, j) \in X_T$ is selected. New values of the rate coefficient k_l , $l = 1, \dots, 8$, are calculated by (3) for the cell state $(i, j) \in X_T$. Then the new values of probabilities p_l , $l = 1, \dots, 8$, are calculated by (2) and one of the substitutions $\theta_l \in \Theta_{CO}(i, j)$, $l = 1, \dots, 8$, is chosen with probability p_l and applied to the cell $(i, j) \in X_{CO}$. Each iteration of the two-layer CA \aleph_S includes one iteration of \aleph_{CO} and one iteration of \aleph_T .

4. A result of the CA simulation of CO oxidation reaction over Pt

The CO oxidation reaction is simulated by means of the two-layer CA \aleph_S with the cellular array size $M_i \times M_j = 320 \times 320$ cells for different values of k_1 and k_6 . The diffusion intensity value is $M_{diff} = 50$. The temperature diffusion rate γ is equal to 0.8. At the initial moment, all the cells states of the main CA \aleph_{CO} are $*_{hex}$, corresponding to a free catalyst surface with a hexagonal structure. Initial cellular arrays of the second layer CA \aleph_T are different for different computing experiments, it is the parameter to be studied. For annihilation of boundary effects, the periodic boundary conditions are used.

In the course of the simulation, the following characteristics are obtained:

1. Concentrations of reagents adsorbed on the catalytic surface: $n(O_{ads})$ and $n(CO_{ads})$, obtained after each iteration as ratio of the amount N of cells with the state O_{ads} or CO_{ads} to the cellular array size:

$$n(CO_{ads}) = \frac{N(CO_{ads}^{1 \times 1}) + N(CO_{ads}^{hex})}{M_i M_j},$$

$$n(O_{ads}) = \frac{N(O_{ads}^{1 \times 1}) + N(O_{ads}^{hex})}{M_i M_j}.$$

2. Intensity of CO_2 formation, $v(\text{CO}_2)$, computed as the amount of interactions between CO_{ads} and O_{ads} per iteration divided by the cellular array size $M_i M_j$:

$$n(v(\text{CO}_2)) = \frac{N(\text{CO}_{\text{ads}} + \text{O}_{\text{ads}})}{M_i M_j}.$$

3. A portion of the surface with cubic and hexagonal structure, $n(1 \times 1)$ and $n(\text{hex})$, calculated after each iteration by the following formulas:

$$n(1 \times 1) = \frac{N(*_{1 \times 1}) + N(\text{CO}_{\text{ads}}^{1 \times 1}) + N(\text{O}_{\text{ads}}^{1 \times 1})}{M_i M_j},$$

$$n(\text{hex}) = \frac{N(*_{\text{hex}}) + N(\text{CO}_{\text{ads}}^{\text{hex}}) + N(\text{O}_{\text{ads}}^{\text{hex}})}{M_i M_j}.$$

The computing experiment is carried out with the same parameters as in [5]: $k_1 = 14.7$ and $k_6 = 56$. As theoretical test for check CA-model the following initial cells states of \aleph_T are considered:

$$(u, (i, j)) : \quad u = \begin{cases} T_c = 480 \text{ K}, & \text{if } i \in [10, 310] \text{ and } j \in [10, 310], \\ T_b = 10 \text{ K}, & \text{otherwise.} \end{cases}$$

Thus, at $t = 0$, the catalyst surface has a high temperature of 480 K in the central 300×300 square and a low temperature close to 0 K on the borders (Figure 2a). Then temperature is gradually equalized on the whole catalyst surface owing to a heat transfer from the heated central part to cold borders.

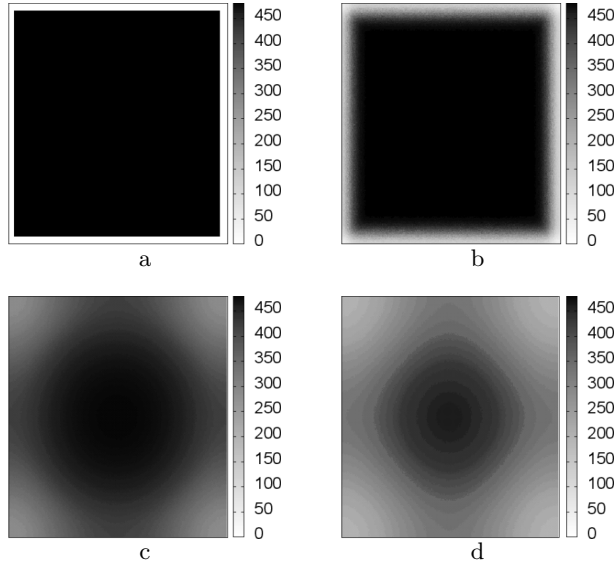


Figure 2. The spatiotemporal distribution of temperature over the catalyst surface: a) at the initial time; b) at the 100th iteration; c) at the 5,000th iteration; and d) at the 8,500th iteration

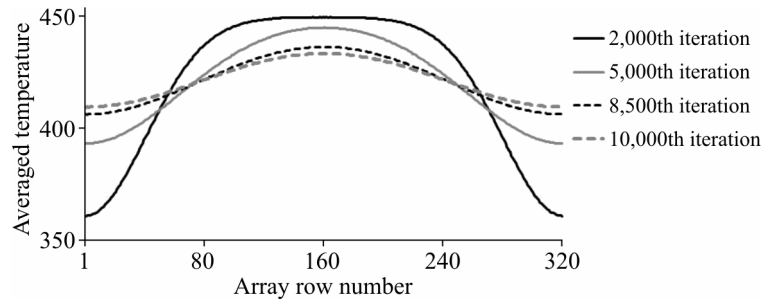


Figure 3. A change in the averaged temperature of the catalyst surface from 2,000th to the 10,000th iteration

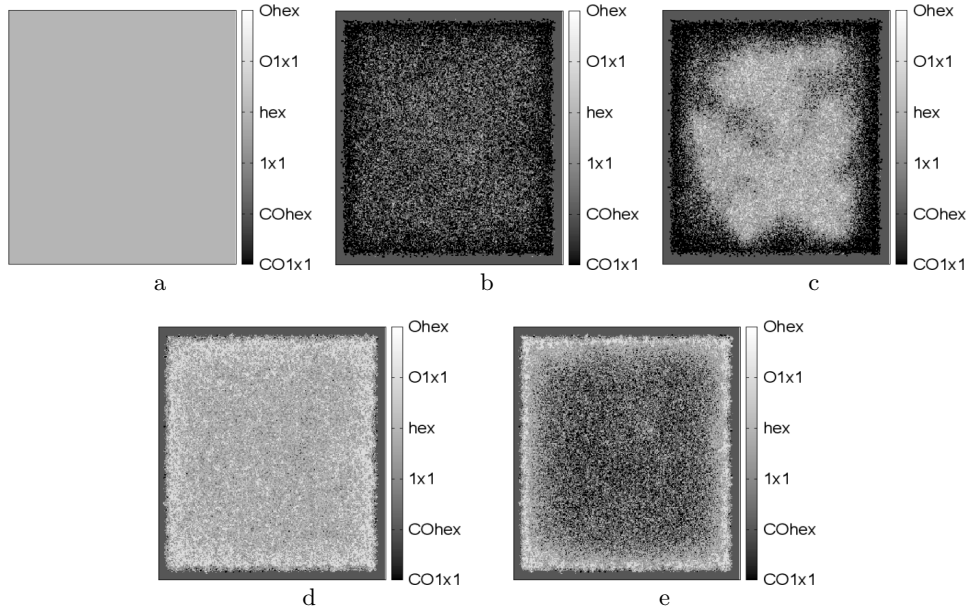


Figure 4. Changes in adsorbed reagents coverages $\text{CO}_{\text{ads}} \leftrightarrow \text{O}_{\text{ads}}$ during the reaction: a) the surface in the hex state (the initial time); b) the surface covered with CO_{ads} (the 30th iteration); c) O_2 adsorption (the 40th iteration); d) the surface covered with O_{ads} (the 55th iteration); and e) the central part of surface covered with CO_{ads} (the 105th iteration)

Heat transfer obtained by \aleph_T evolution is presented in Figure 2b–d. Here, the black color represents heat, the white color representing cold. A change in the averaged temperature during the evolution is shown in Figure 3. The averaged temperature is calculated for each column of the cellular array as mean value of the cells states in the column.

As a result of the CA simulation with the two-layer CA \aleph_S , the following dynamics of CO oxidation reaction is observed (Figure 4).

In the beginning, the platinum surface is in the hex state (see Figure 4a) with temperature distribution shown in Figure 2a. The rate coefficients values are greater for the heated surface. Hence, the oxidation reaction occurs only on the heated central square, whereas on the borders with a low temperature reaction does not occur. Since the probability of the CO adsorption at the hexagonal active centers is greater than that of the O₂ adsorption, CO_{ads} accumulating on the surface (see Figure 4b). Simultaneously with CO_{ads} accumulation, due to the phase reconstruction of the surface (stage s_4), 1×1 surface portion increases. Since probability of O₂ adsorption on 1×1 surface exceeds probability of CO adsorption, oxygen is adsorbed on the catalyst surface (see Figure 4c) and interacts with CO_{ads}. Due to this interaction, a portion of the vacant active centers $*_{1 \times 1}$ increases. However, a free 1×1 surface is unstable, $*_{1 \times 1}$ centers are reconstructed in $*_{\text{hex}}$ owing to spontaneous phase transition (stage s_5). An increase of hex surface portion again creates favourable conditions for CO adsorption.

Meanwhile, by this time the temperature of initially heated square borders decreases owing to the heat transfer (see Figure 2b) and, consequently, the rate coefficients values decrease for these centers. Therefore, on the sur-

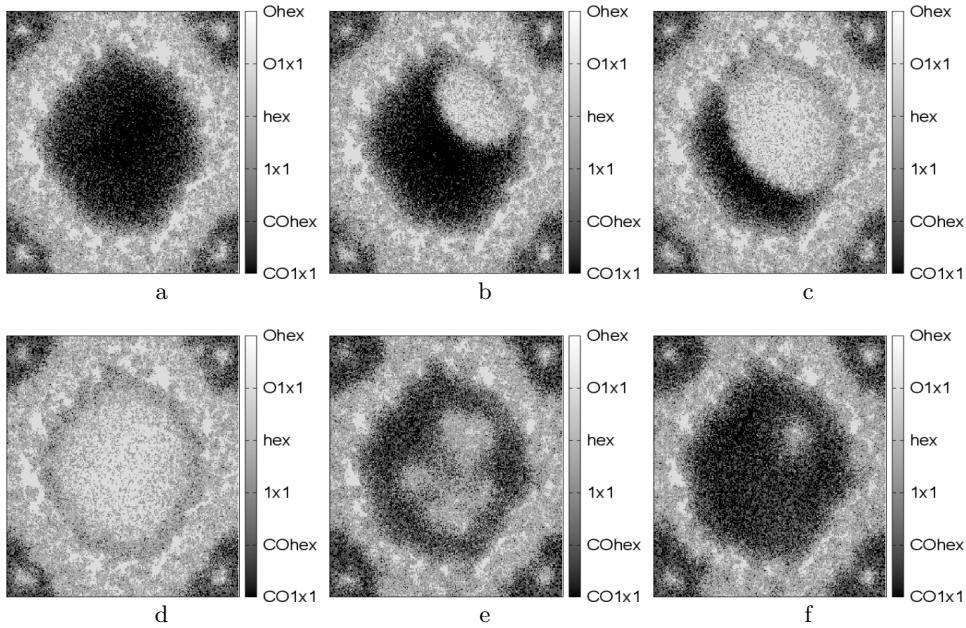


Figure 5. Changes in coverages $\text{CO}_{\text{ads}} \leftrightarrow \text{O}_{\text{ads}}$ in the catalyst center: a) CO_{ads} circle in the catalyst center; b) formation of O_{ads} wave into CO_{ads} circle; c) propagation of O_{ads} wave into CO_{ads} circle, d) O_{ads} circle in the catalyst center; e) propagation of CO_{ads} into O_{ads} circle; and f) formation of CO_{ads} coverage into O_{ads} circle

face borders reconstruction of $*_{1\times 1}$ into $*_{\text{hex}}$ centers does not occur. Thus, on the initially heated square borders, O_{ads} accumulates and does not desorb (see Figure 4d). Whereas on the heated central square CO adsorption occurs again (see Figure 4e), and oscillations of adsorbed reagents coverages are observed.

When the surface temperature is equalized over the catalyst (see Figure 2c), the catalyst area, where the reaction occurs, decreases. Changes in the reagents coverage of CO_{ads} into O_{ads} and vice versa occur only into the circle at the catalyst center (Figure 5). The rest of the surface is mainly covered with O_{ads} .

Further, due to the heat transfer, the temperature of the whole surface becomes lower than it is needed for oscillation emerging. Therefore, oscillations disappear and the surface becomes covered with CO_{ads} .

Oscillations of the reagents concentrations $n(\text{CO}_{\text{ads}})$, $n(\text{O}_{\text{ads}})$, $n(v(\text{CO}_2))$, $n(1\times 1)$ and $n(\text{hex})$ are shown in Figure 6.

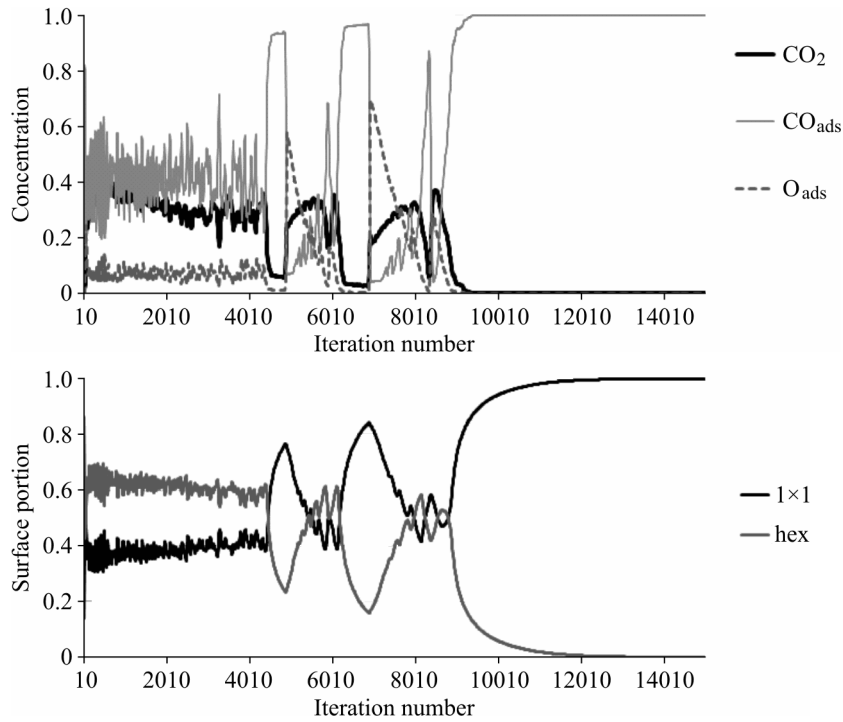


Figure 6. The oscillation character of CO oxidation reaction over Pt: concentration of CO_{ads} , O_{ads} and intensity of CO_2 formation (top) and a portion of the surface with 1×1 and hex structures (bottom)

5. Conclusion

The two-layer CA model for simulating the CO oxidation reaction over the surface Pt with allowance for the catalyst surface temperature is proposed and investigated.

It was found that CA \aleph_S demonstrates oscillations of adsorbed reagents concentrations, CO₂ formation intensity, and a portion with 1×1 and hex surface structures. The oscillations are accompanied by different chemical waves on the modeling surface. The oxidation reaction dynamics changes with changing the surface temperature owing to the heat transfer. The two-layer CA makes possible to simulate and study the reaction behavior for a variable catalyst temperature.

References

- [1] Wolfram S. Cellular Automata as Simple Self-Organizing Systems. — 1982. — (Preprint / Caltech; CALT-68-938). — <http://www.stephenwolfram.com/publications/articles/ca/82-cellular/index>.
- [2] Young D.A. A local activator-inhibitor model of vertebrate skin patterns // Theory and applications of cellular automata. Advanced series on complex systems / S. Wolfram, ed. — World Scientific Publishing, 1986. — No. 1. — P. 320–327.
- [3] Bandman O.L. Cellular automatic models of spatial dynamics // System Informatics. Methods and Models of Modern Programming. — 2006. — Vol. 10. — P. 59–113.
- [4] Vanag V.K. Dissipative Structures in Reaction-Diffusion Systems / Regular and Chaotic Dynamics. — Moscow-Izhevsk: Institute of Computer Researches, 2008.
- [5] Matveev A.V., Latkin E.I., Elokhin V.I., Gorodetskii V.V. Monte Carlo model of oscillatory CO oxidation having regard to the change of catalytic properties due to the adsorbate-induced Pt(100) structural transformation // J. Molecular Catalysis A: Chemical. — 2001. — Vol. 166. — P. 23–30.
- [6] Elokhin V.I., Sharifulina (Kireeva) A.E. Simulation of heterogeneous catalytic reaction by asynchronous cellular automata on multicomputer // LNCS. — Springer, 2011. — Vol. 6873. — P. 204–209.
- [7] Matveev A.V., Latkin E.I., Elokhin V.I., Gorodetskii V.V. Application of statistical lattice models to the analysis of oscillatory and autowave processes in the reaction of carbon monoxide oxidation over platinum and palladium surfaces // Kinetics and Catalysis. — 2003. — Vol. 44, No. 5. — P. 692–700.
- [8] Gorodetskii V.V., Elokhin V.I., Bakker J.W., Nieuwenhuys B.E. Field electron and field ion microscopy studies of chemical wave propagation in oscillatory reactions on platinum group metals // Catalysis Today. — 2005. — Vol. 105. — P. 183–205.

- [9] Imbihl R., Cox M.P., Ertl G. Kinetic oscillations in the catalytic CO oxidation on Pt(100): Theory // *J. Chemical Physics*. — 1985. — Vol. 83, No. 4. — P. 1578–1587.
- [10] Bandman O.L. Using multi core computers for implementing cellular automata systems // *Proceedings of Parallel Computing Technologies*. — Springer, 2011. — P. 140–151. — (LNCS; 6873).
- [11] Medvedev Yu.G. Multi-particle cellular-automata models for diffusion simulation // *LNCS*. — Springer, 2010. — Vol. 6083. — P. 204–211.

